Characterisation of extracellular vesicles directly in diluted canine and human blood and plasma for therapeutic plasma

Berry Maxence[1,2], Hočevar Matej [3], Kisovec Matic [4], Arko Matevž [1], Jan Zala [1], Brložnik Maja [1], Korenjak Boštjan [1], Romolo Anna [1], Bedina Zavec Apolonija [4], Iglič Aleš [1], Erjavec Vladimira [1], Svete Nemec Alenka [1], Kralj-Iglič Veronika [1]

[1] University of Ljubljana, Ljubljana, Slovenia; [2] University of Poitiers, Poitiers, France; [3] Institute of Metals and Technology, Ljubljana, Slovenia; [4] National Institute of Chemistry, Ljubljana, Slovenia

Results

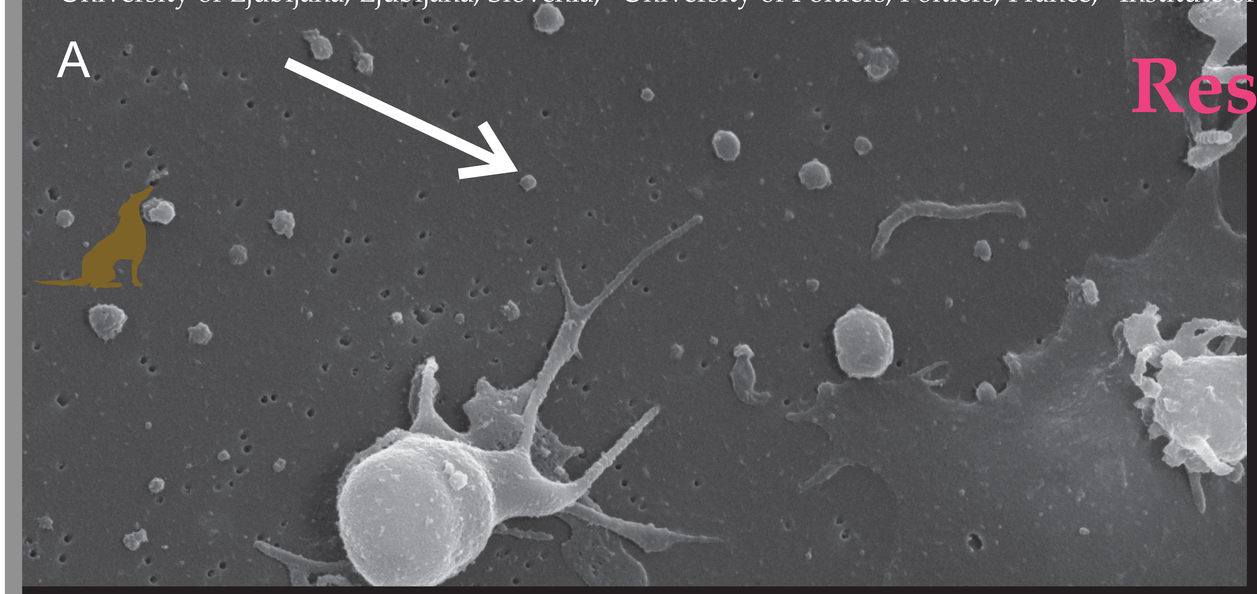

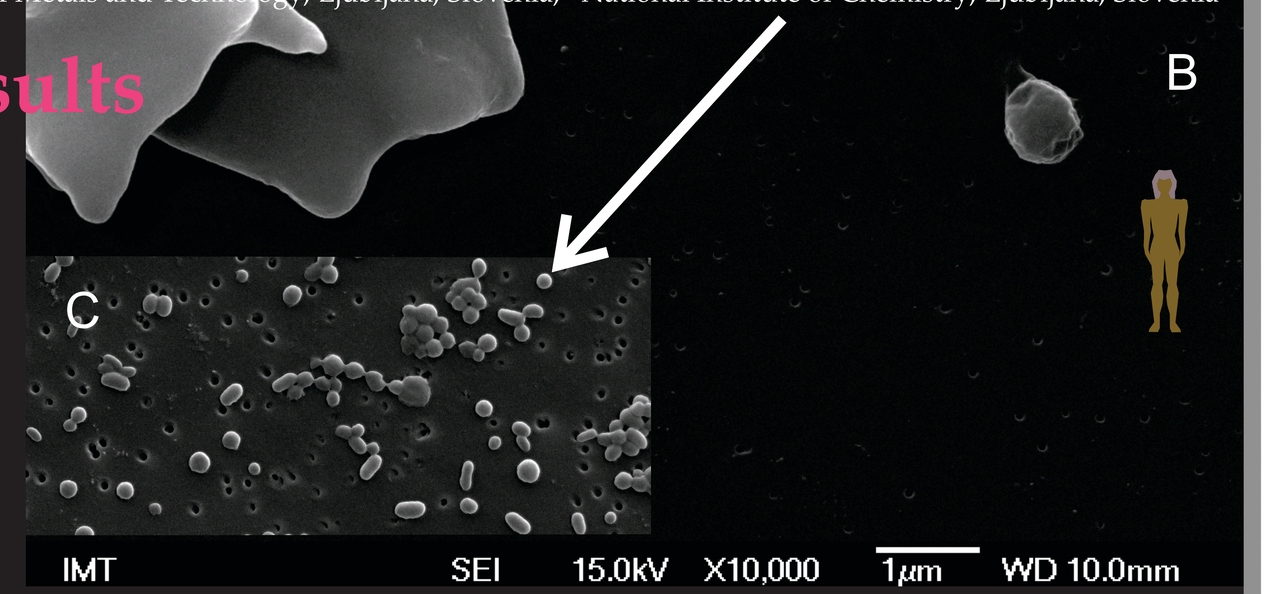

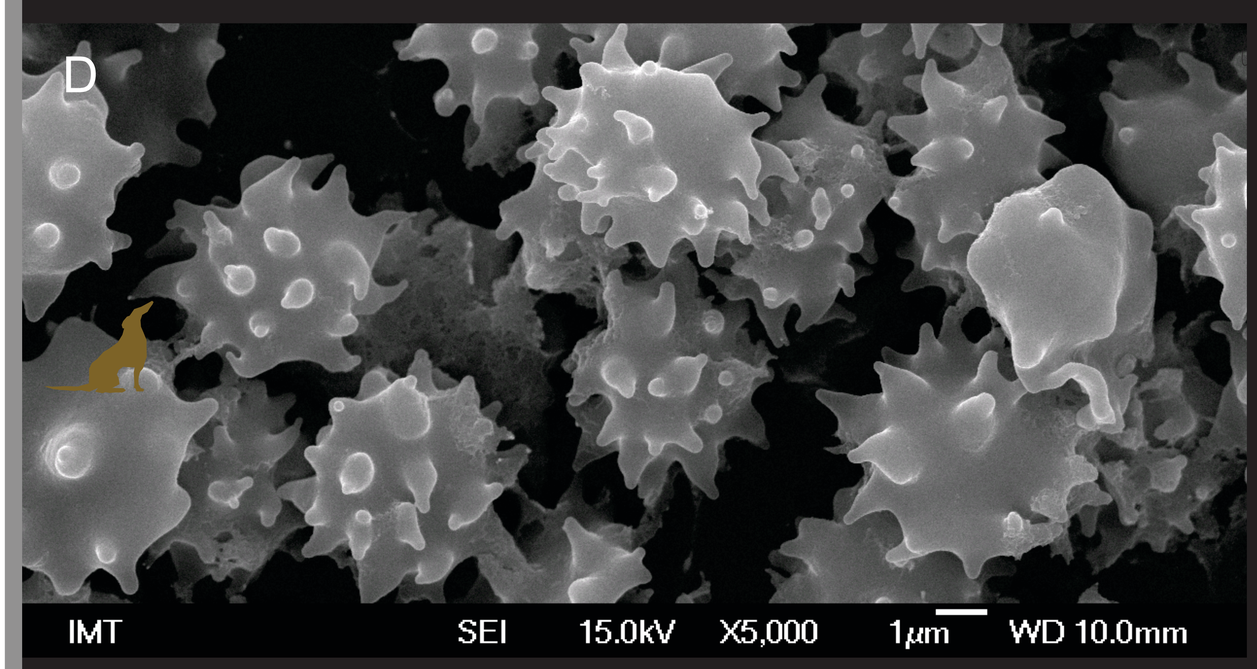

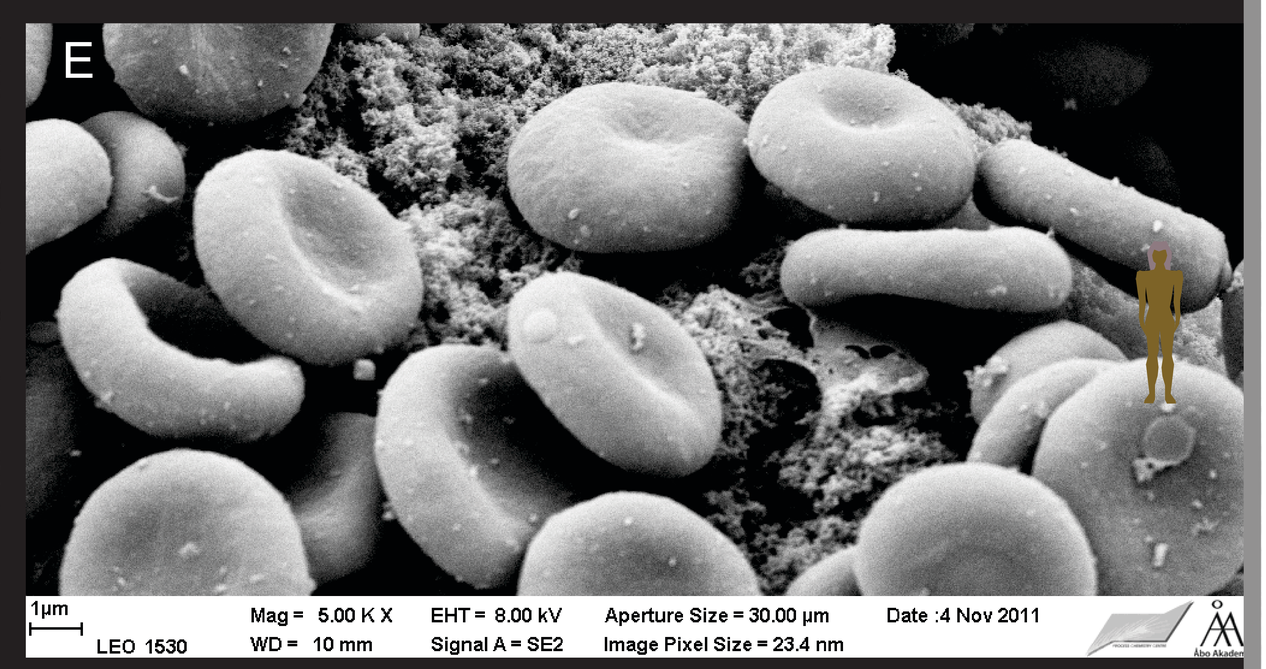

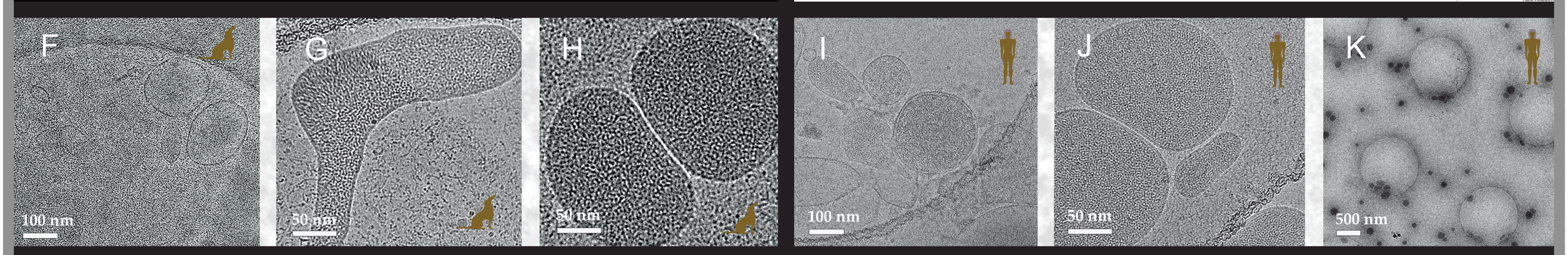

Figure 1. Scanning electron microscope images of A: EVs from canine plasma, B,C: human plasma, D: canine blood, E: human blood. Cryo-EM images of F: EVs from canine plasma, G,H: EVs from canine blood, I: EVs from human plasma, J,K: EVs from human blood.

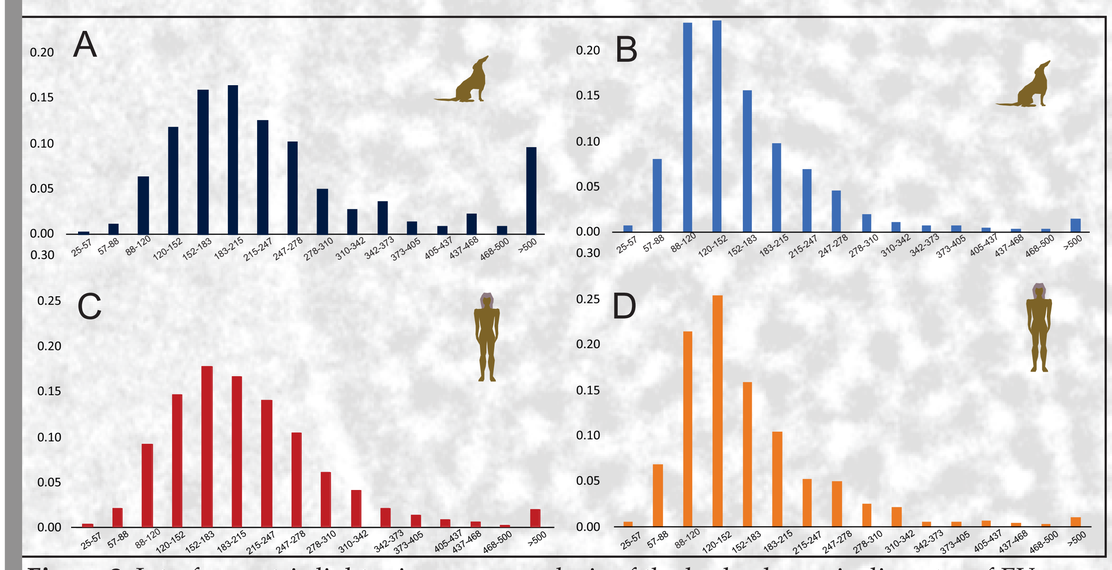

Figure 2. Interferometric light microscopy analysis of the hydrodynamic diameter of EVs. A: canine blood, B: canine plasma, C: human blood, D: human plasma.

Table 1. Number density of EVs.

		Average Number Density of EVs in Blood ($10^6/\mu L$)	Average Number Density of EV's in Plasma ($10^6/\mu L$)
Canine	Dog 1	73	38
	Dog 2	104	5
	Dog 3	232	111
Human	Human 1	128	19
	Human 2	108	63
	Human 3	203	70

Table 2. Statistical significance of the differences between hydrodynamic diameters of EVs in different types of samples.

p (T Test)	Canine Plasma	Human Blood	Human Plasma	N=960
Canine Blood N=367	$<10^{-6}$	$<10^{-6}$	$<10^{-6}$	N: number of EVs measured
Canine Plasma N=1320		$<10^{-6}$	$<10^{-6}$	
Human Blood N=1684			$<10^{-6}$	

Interferometric light microscopy enables high throughput assessment of number density and hydrodynemic diameter of EVs in blood and in plasma (no filtering). There were more EVs in blood than in plasma. Canine and human EVs are similar in shape, size and number density on the population level, but there are inter-individual variations.

Methods

2.1. Sampling of blood

Canine blood was taken from two expired transfusion bags and one healthy donor. Blood from transfusion bags was aliquoted into 3 mL tubes (Vacuette 454241, Greiner Bio-One GmbH, Kremmunster, Austria). Human blood was donated by 1 female and 2 male donors without record of disease. Collection of blood was established in the morning after fasting for a minimum of 12 h overnight. A G21 needle (Microlance, Becton Dickinson, Franklin Lakes. NJ, USA) and 2.7 mL evacuated tubes with trisodium citrate (BD Vacutainers, 367714A, Becton Dickinson, Franklin Lakes, NJ, USA) were used. Fresh blood was processed within 1 hour of sampling. While waiting to be centrifuged, the samples were gently mixed on a carousel at room temperature. To prepare plasma, blood was centrifuged in the tubes in which it was sampled at 18 °C and 300g in the Centric 400R centrifuge (Domel, Železniki, Slovenia) with swinging rotor RS4/100. The time of centrifugation to yield maximal concentration of platelets in plasma was estimated by a mathematical model (Božič et al., Enrichment of plasma in platelets and extracellular vesicles by the counterflow to erythrocyte settling. Platelets. 33 (2022) 592–602). The velocity of the movement of the erythrocyte boundary was assessed by centrifugation of blood for t_{test} = 5 minutes. The length of the acquired plasma l_{test}, the distance between the bottom of the tube and the centrifuge rotor axis x_{max} and the distance between the level of the sample and the centrifuge rotor axis x_{min} in horizontal position were measured by a ruler. Parameter τ_{test} for individual sample was estimated by $\tau_{test} = \ln(1 + l_{test}/x_{min})$. Parameter for the individual blood was calculated by $\tau_{opt} = \ln(1 + L_{test}/x_{min})/(X\, t_{test})$, where X is the multiplicity of g in centripetal acceleration of the centrifuge rotor. The optimal centrifugation time was calculated by $t_{opt} = \ln(x_{max}/x_{min})/(2\omega X)$. Then, blood was centrifuged at 18 °C and 300 g (X = 300) for t_{opt}.

2.2. Interferometric light microscopy (Romolo, A.; et al., Assessment of Small Cellular Particles from Four Different Natural Sources and Liposomes by Interferometric Light Microscopy. Int. J. Mol. Sci. 2022, 23, 15801. https://doi.org/10.3390/ijms232415801)

The average hydrodynamic diameter (D_h) and the number density of EVs were determined by ILM using Videodrop (Myriade, Paris, France). Signal from the medium (physiological saline) was under the detection limit. The threshold value of 3.8 was used. Seven microliters of sample were placed between cover glasses and illuminated by 2 W of blue LED light. The light scattered on the particle was imaged by a bright-field microscope objective and allowed to interfere with the incoming light (**Figure 3**). The image was recorded by a complementary metal-oxide-semiconductor high-resolution high-speed camera. Interference enhances the information in the scattered light. However, although the intensity of the interference signal is about 3 orders of magnitude higher than the intensity of the scattered light, the intensity of the incident light is about 3 orders of magnitude higher than the intensity of the interference signal. Therefore, the contribution of the incident light was subtracted from the detected image. The obtained pattern, which includes contrasting black and white spots, was recognized as a particle, and its position in the sample was assessed. The number density of the particles is the number of detected particles within the detected volume, which depends on the microscope characteristics and the particles' size. The typical detection volume was 15 pL. Hydrodynamic diameter D_h was estimated by tracking the position of the imaged particle within the recorded movie. It was assumed that particles undergo Brownian motion due to collisions with surrounding particles. The motion is random, but the kinetic energies and momenta of the particles reflect the emperature of the sample. Particles with smaller masses move within a larger volume than particles with larger masses. The diffusion coefficient D of the motion of the particle is taken to be proportional to the mean square displacement d of the particle between two consecutive frames taken in the time interval Δt, $\langle d^2(\Delta t)\rangle = \langle 4D\,\Delta t\rangle$, while the hydrodynamic diameter was estimated by assuming that the particles were spherical and using the Stokes–Einstein relation $D_h = kT/3\pi\eta D$. Each particle that was included in the analysis was tracked and processed individually, and the respective incident light signal was subtracted from each image. Processing of the images and the movies was performed by using the associated software, QVIR 2.6.0 (Myriade, Paris, France). We measured samples in triplicates. We diluted blood with physiological saline 200 times and plasma 50 times.

2.3. Scanning Electron Microscopy

Samples were placed on 0.05-micron mixed-cellulose-esters' filters (Sterlitech, Auburn, AL, USA) and incubated in 39.3 mM double distilled water solution of OsO_4 for 2 h. Then they were washed 3 times with distilled water (10 min each), dehydrated in graded series of ethanol (30%, 50%, 70%, 80%, 90%) and absolute ethanol, each step 10 min. Absolute ethanol was replaced twice. Then they were washed in hexamethyldisilazane (mixed with absolute ethanol; 30% and 50%) and in absolute hexamethyldisilazane, each step 10 min. The samples were left to dry in air overnight. For examination under JSM-6500F Field Emission Scanning Electron Microscope (JEOL Ltd., Tokyo, Japan), the samples were sputtered with Au/Pd (PECS Gatan 682). For SEM, blood was washed with physiological saline.

2.4. Cryogenic Transmission Electron Microscopy

C-flat™ 2/2, 200 mesh holey carbon grids (Protochips, Morrisville, NC, USA) were glow discharged: 20 mA, 60 s, positive polarity, air atmosphere (GloQube® Plus, Quorum, Laughton, UK). Then, 3 μL of the sample was applied to the grid, blotted, and vitrified in liquid ethane on Vitrobot Mark IV (Thermo Fisher Scientific, Waltham, MA, USA). Vitrobot conditions were set to 100% relative humidity, 4 °C, blot force: 2 and blot time: 7 s. Samples were visualized under cryogenic conditions using a 200 kV Glacios microscope with a Fal-con 3EC detector (Thermo Fisher Scientific, Waltham, MA, USA).

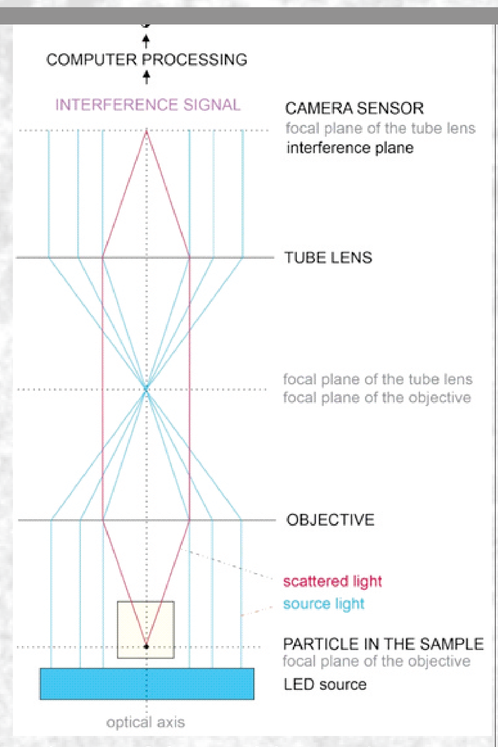

Figure 3. Scheme of the Interferometric light microscopy.

Presented at Small New World 2.0; Joint Meeting of ASEV, HSEV, SiNEV and SrbEV, September 4-5, 2023 in Graz, Austria.

www.lkbf.si
veronika.kralj-iglic@zf.uni-lj.si
maxence.berry.pro@gmail.com

Acknowledgements : This research was supported by Slovenian Research Agency grants: J3-3066, P3-0388, P1-0391, P2-0132, P2-0232, J2-4447, J2-4427 and L3-2621, National Research, Development and Innovation Office (Hungary) SNN 138407 and Amexio who financially contributed to the internship of the first author. We thank Vid Šuštar and Henry Hagerstrand from Abo Akademi University, Finland for imaging of human erythrocytes (Figure 1E).